Elastic constants and chemical bonding of $LaNi_5$ and $LaNi_5H_7$ by first principles calculations

2003 J. Phys.: Condens. Matter 15 6549

(http://iopscience.iop.org/0953-8984/15/38/021)

INSTITUTE OF PHYSICS PUBLISHING JOURNAL OF PHYSICS: CONDENSED MATTER

J. Phys.: Condens. Matter **15** (2003) 6549–6561 PII: S0953-8984(03)60822-2

Elastic constants and chemical bonding of $LaNi_5$ and $LaNi_5H_7$ by first principles calculations

Kazuyoshi Tatsumi[1,3], Isao Tanaka[1], Katsushi Tanaka[1], Haruyuki Inui[1], Masaharu Yamaguchi[1], Hirohiko Adachi[1] and Masataka Mizuno[2]

[1] Department of Materials Science and Engineering, Kyoto University, Sakyo, Kyoto 606-8501, Japan
[2] Department of Materials Science and Engineering, Osaka University, Suita, Osaka 565-0871, Japan

E-mail: kazu@cms.MTL.kyoto-u.ac.jp

Received 13 March 2003
Published 12 September 2003
Online at stacks.iop.org/JPhysCM/15/6549

Abstract

Elastic constants of $LaNi_5H_7$ and $LaNi_5$ are calculated by a first principles pseudopotential method using plane-wave basis sets. Some extra calculations using model clusters were made in order to discuss the magnitude of chemical bondings. Inner displacements associated with all deformation modes are taken into account. Elastic constants are smaller and more isotropic in the hydride than those in the host. The electronic mechanism to determine the change in the elastic properties is investigated from the viewpoint of chemical bonding. Strong Ni–H bonds are formed in $LaNi_5H_7$ at the expense of Ni–Ni bonds. They play key roles in determining the elastic properties. The isotropic distribution of the Ni–H bonding charge in $LaNi_5H_7$ should be responsible for the isotropic elastic constants. Hydrogen atoms are found to relax considerably during the deformation to maintain the Ni–H bond length. When the inner displacements are ignored, the elastic constants of $LaNi_5H_7$ are as large as those of $LaNi_5$. However, the remarkable displacement of hydrogen atoms during the elastic deformation plays an essential role in softening by hydrogenation.

1. Introduction

Energy conversion/storage devices fabricated using metal hydrides play very important roles in modern technology in which clean and efficient energy production is required. $LaNi_5$-based alloys have been known to show good hydrogen storage characteristics suitable for a wide range of applications such as negative electrodes for rechargeable Ni–metal hydride batteries [1–3]. Although there have been numerous reports on the engineering aspects of

[3] Author to whom any correspondence should be addressed.

0953-8984/03/386549+13$30.00

these alloys, fundamental information is still very limited. For example, the crystal structure of the full hydride, $LaNi_5H_{6-7}$ has not been definitively established by neutron diffraction experiments [4]. In our previous report, we systematically calculated various phases of the $LaNi_5$–H system [5]. Atomic structures of the full hydride, $LaNi_5H_7$, were examined in detail. The preferred hydrogen site and its local environment in the primary solid solution were also investigated. Theoretical formation energies of these phases were discussed, together with other phases of intermediate compositions. Although elastic constants are very important for designing materials from engineering viewpoints, no measurements on any $LaNi_5$ hydrides have thus far been reported. Only the elastic constants of $LaNi_5$ have been reported by Tanaka *et al* [6] for a single crystal using a resonance vibration method. $LaNi_5$ samples are usually pulverized during the hydrogenation process because of the huge internal strain induced by the volume expansion. No single crystals of the hydrides sufficiently large for elastic measurements have been available because of the pulverization. Reliable theoretical calculations that reveal the elastic properties of the hydrides have therefore been strongly desired.

The present study aims to evaluate the elastic constants of the full hydride phase, $LaNi_5H_7$. Although the electronic structure of $LaNi_5$–H systems has thus far been calculated repeatedly [5, 7–14], no elastic property has been described by means of any quantum mechanical calculations. In the present study, we report theoretical elastic constants of $LaNi_5H_7/LaNi_5$ for the first time. Then we discuss the atomic/electronic mechanism to determine the change in the elastic properties due to the hydrogenation.

2. Computational details

A plane-wave basis pseudopotential (PW-PP) method [15][4] has been employed, which is the same as the one used in [5]. Atomic structures were fully optimized for $LaNi_5$ and $LaNi_5H_7$ as described in the report [5]. Elastic constants were calculated using crystal parameters optimized in [5]. $LaNi_5$ exhibits a hexagonal structure with the space group $P6/mmm$ ($CaCu_5$-type structure) [16]. We use a model of $LaNi_5H_7$ having the hypothetically ordered structure. Because the space group of the hydride was hardly determined uniquely within the computational accuracy, we have chosen a structure with the space group $P6_3mc$, for simplicity. Detailed results on the atomic structures of hydrides are shown in [5].

Electron exchange–correlation effects were taken into account using the Perdew–Wang form of the generalized gradient approximation (GGA) [17]. In order to reduce the number of plane waves, ultrasoft pseudopotentials [18] were employed for all ions, i.e., La, Ni and H. The pseudopotentials were constructed for neutral atoms. The La-4f orbital was therefore not included. The ultrasoft potential for H was recently reported to be useful for an accurate description of H in complex solids [19]. With these pseudopotentials, the plane-wave cutoff, E_{cut} was chosen to be 380 eV. The convergence of the elastic constants is smaller than 2% up to $E_{\mathrm{cut}} = 800$ eV. The $\boldsymbol{k}$-points used for numerical integration were chosen at the mesh points by Monkhorst and Pack's scheme [20]. The mesh points corresponded to 75 and 32 $\boldsymbol{k}$-points throughout the entire Brillouin zone (BZ) of $LaNi_5$ and $LaNi_5H_7$, respectively. Convergence of the total energies with respect to the number of $\boldsymbol{k}$-points was verified up to 196 and 96 $\boldsymbol{k}$-points throughout the entire BZ of $LaNi_5$ and $LaNi_5H_7$. It was found to be better than 0.01 eV/unit formula. The convergence of the elastic constants was found to be smaller than 0.2% up to the above $\boldsymbol{k}$-points. Spin polarization was not taken into account because the effect of the spin polarization on the total energy was well below the computational accuracy. The quantum nuclear effect of hydrogen was disregarded throughout the present study.

[4] The present calculations were performed using the CASTEP program code (Accerlys, Inc., San Diego, CA).

3. Results

The internal energy of a crystal under an infinitesimal strain of α, $E(V, \alpha)$, can be expressed as [21, 22]

$$E(V,\alpha) = E(V_0,\alpha) + V_0\left(\sum_i \tau_i\xi_i\alpha_i + \tfrac{1}{2}\sum_{i,j} C_{ij}\alpha_i\xi_i\alpha_j\xi_j\right) + \mathrm{O}(\alpha^3), \tag{1}$$

where V_0 denotes the volume of the unstrained system. We use the Voigt notation in equation (1) whereby xx is replaced by 1, yy by 2, zz by 3, yz (and zy) by 4, xz (and zx) by 5, and xy (and yx) by 6. The factors ξ_i have the conventional meaning used to introduce the Voigt notation, and are unity if the Voigt number is 1, 2, or 3, and 2 if the Voigt number is 4, 5, or 6. τ_i is an element in the stress tensor. There are five independent elastic constants for a hexagonal crystal, i.e., C_{11}, C_{12}, C_{13}, C_{33} and C_{44}. We need a set of five independent total energy calculations, in principle. Elastic constants can also be calculated from quantum mechanical forces obtained under given stresses, which may be computationally less demanding. In the present study, however, crystals were deformed in six different ways to obtain total energy as a function of strain. The elastic constant for each deformation mode was then obtained from the curvature of the total energy-strain curve. Five elastic constants were obtained on five deformation modes. The sixth deformation mode was used to check the numerical accuracy of the five constants. In addition to the energy, the magnitude of atomic displacements associated with all deformation modes were examined in detail.

The first deformation mode can be described as

$$\begin{pmatrix} 1+\alpha & 0 & 0 \\ 0 & 1+\alpha & 0 \\ 0 & 0 & 1 \end{pmatrix}. \tag{2}$$

This mode changes the size of the basal plane while the c-axis remains. The elastic constant obtained for this mode corresponds to $C_{11} + C_{12}$. The second mode stretches the c-axis while the basal plane remains, i.e.,

$$\begin{pmatrix} 1 & 0 & 0 \\ 0 & 1 & 0 \\ 0 & 0 & 1+\alpha \end{pmatrix}. \tag{3}$$

The elastic constant corresponds to $C_{33}/2$ for this mode. The third deformation increases the a-axis and decreases the b-axis. The matrix is

$$\begin{pmatrix} 1+\alpha & 0 & 0 \\ 0 & 1-\alpha & 0 \\ 0 & 0 & 1 \end{pmatrix}, \tag{4}$$

which corresponds to $C_{11} - C_{12}$. The fourth mode expressed by

$$\begin{pmatrix} 1 & 0 & 0 \\ 0 & 1 & \alpha \\ 0 & \alpha & 1 \end{pmatrix}, \tag{5}$$

corresponds to $2C_{44}$, which is equivalent to $2C_{55}$. The fifth deformation expressed as

$$\begin{pmatrix} 1+\alpha & 0 & 0 \\ 0 & 1+\alpha & 0 \\ 0 & 0 & 1-2\alpha \end{pmatrix}, \tag{6}$$

corresponds to $C_{11} + 2C_{33} + C_{12} - 4C_{13}$. Five independent constants can be determined by the deformations given by equations (2)–(6). In addition to these five modes, we have calculated the bulk modulus, B, for the deformation given by

Table 1. Elastic constants of $LaNi_5$ and $LaNi_5H_7$ in GPa. Theoretical elastic constants with and without inner displacements are showed in the left (rigid model) and right (+inner displacement) columns, respectively. The bulk modulus, B, was calculated from the deformation given by equation (7).

	$LaNi_5$			$LaNi_5H_7$	
	Theory			Theory	
Elastic Constants	Rigid model	+inner displacement	Experiment[a]	Rigid model	+inner displacement
B	143	143	127	140	130
C_{11}	218	218	190	230	190
C_{33}	266	—	230	231	188
C_{12}	107	108	96.9	107	97
C_{13}	93	—	84.8	96	108
C_{44}	67	67	59.9	52	35
C_{66}	56	55	46.6	61	46

[a] Reference [6].

$$\begin{pmatrix} 1+\alpha & 0 & 0 \\ 0 & 1+\alpha & 0 \\ 0 & 0 & 1+\alpha \end{pmatrix}. \tag{7}$$

B is not independent of the above five equations, and is expressed by

$$B = \frac{2}{9}\left(C_{11} + C_{12} + 2C_{13} + \frac{C_{33}}{2}\right). \tag{8}$$

We calculated B using equation (8) and using the sixth deformation mode in order to confirm the computational accuracy. Theoretical elastic constants were determined from seven data points with different α in the range of $|\alpha| \leqslant 1\%$. The range was chosen so as to make the $O(\alpha^3)$ term in equation (1) negligible and the elastic energy increment with α computationally reliable. Elastic constants were also calculated with α in the range of $|\alpha| \leqslant 2\%$. We found the difference in the elastic constants to be smaller than 2%.

When a crystal of complicated structure is deformed, not only its cell constants but also some internal parameters can be changed within the space group of the deformed crystal. The displacement of the internal parameters has been pointed out to contribute non-negligibly to the calculation of elastic constants in some systems [21, 23–29]. We will hereafter refer to such displacements as inner displacements. In the present study, elastic constants were calculated in two ways, i.e. with and without the inner displacements. The inner displacements were limited so that the space groups of the deformed crystals with and without relaxation were identical. For $LaNi_5$, the optimization of the internal parameters was possible only for the deformation modes of C_{44} and $C_{11} - C_{12}$. On the other hand, for $LaNi_5H_7$, the relaxation can be taken into account for all deformation modes. The geometry was optimized using the BFGS technique [30] such that the forces on the atoms derived from the Hellman–Feynman theorem were smaller than 0.05 eV $Å^{-1}$.

Theoretical elastic constants obtained in the present study are summarized in table 1 together with previously reported experimental values for $LaNi_5$ [6]. B has been calculated in two ways, i.e., using equations (7) and (8). The two values agree with each other within an error of 0.3 and 2.2% for $LaNi_5$ and $LaNi_5H_7$. Experimental values were obtained at room temperature using 46 resonance frequencies ranging from 400 to 1800 kHz, by the rectangular parallelepiped resonance method [6]. Errors associated with the experiments were smaller than 1%. Although the theoretical elastic constants are greater than the experimental values

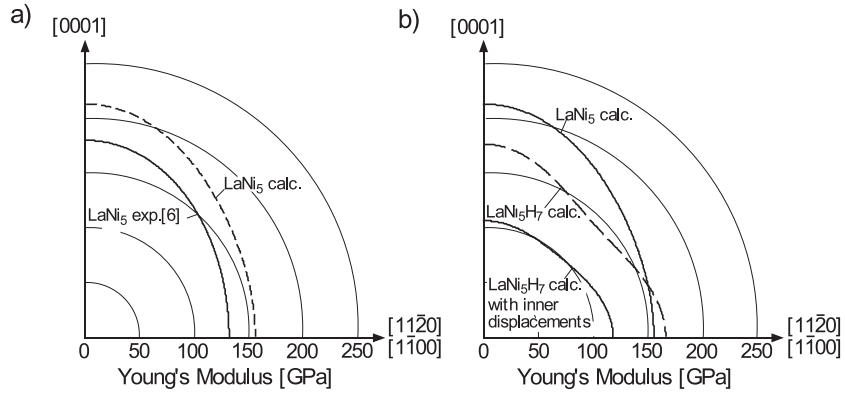

Figure 1. Orientational dependence of Young's moduli: (a) $LaNi_5$ by theory and experiment. The experimental one is from [6]. (b) $LaNi_5H_7$ in comparison with $LaNi_5$. For $LaNi_5H_7$, both the results with and without inner displacements are presented.

by 10–18%, the relative C_{ij} values agree satisfactorily. The reason for the discrepancy in the absolute values is not fully understood. There may be some temperature dependence; the values at room temperature may be 5–10% smaller than the values at zero temperature, in analogy to Ti and Ti_3Al reported previously by Tanaka and Koiwa [31].

Two points can be noteworthy from table 1.

(1) Inclusion of inner displacements significantly reduces most of the C_{ij} s in $LaNi_5H_7$, whereas no significant changes can be noted for $LaNi_5$.
(2) The magnitude of anisotropy among C_{ij} s differs between $LaNi_5$ and $LaNi_5H_7$.

In $LaNi_5$, C_{33} is larger than C_{11}, while they are almost the same in the hydride. C_{44} is larger than C_{66} in $LaNi_5$, while the tendency is reversed in the hydride. These trends can be seen in both cases with and without inner displacements. C_{33} and C_{11} are resistances to tensile or compressive deformation along the z- and x-directions, respectively. C_{44} and C_{66} are resistances to shear on the basal plane and that along the a-direction on a prism plane, respectively. The ratios of C_{33}/C_{11} and C_{44}/C_{66} larger than unity in $LaNi_5$ indicate strong elastic anisotropy along c-axis. The anisotropy is less significant in the hydride.

These two features can be visualized by plotting the orientation dependence of Young's modulus calculated according to the following equation [32]:

$$E_Y(\theta) = \frac{1}{(1-\cos^2\theta)^2 S_{11} + \cos^4\theta S_{33} + \cos^2\theta(1-\cos^2\theta)(2S_{13}+S_{44})}, \quad (9)$$

where S_{ij} are elastic compliance constants and θ is the angle between the c-axis and any arbitrary direction. As can be seen in figure 1, the amplitude of $E_Y(\theta)$ of $LaNi_5H_7$ is markedly decreased due to the inner displacements associated with the deformation. However, the orientational dependence of $E_Y(\theta)$ of $LaNi_5H_7$ with and without relaxation is almost the same. Young's modulus for the c-axis direction ($\theta = 0°$) is not substantially different from that at $\theta = 90°$ in $LaNi_5H_7$. It shows a small hollow at $\theta = 45°$. This small hollow is due to the fact that C_{44} becomes smaller than C_{66} by hydrogenation. On the other hand in $LaNi_5$, Young's modulus is more anisotropic: it is approximately 30% greater for $\theta = 0°$ than for $\theta = 90°$. In the next section, we will discuss the causes of these features. First, we will investigate the electronic mechanism behind the difference in elastic anisotropy between the two crystals. Then, the effect of inner displacements on elastic constants will be examined.

Finally, the theoretical results are discussed from the viewpoint of chemical bondings, on the basis of first principles molecular orbital calculations using model clusters.

Bereznitsky *et al* [33] reported a rough estimation for the ratio of elastic constants between $LaNi_5$ and its hydride from the heat capacity of the hydride using the Debye theory. They estimated the ratio to be 0.46. Although the tendency that the hydride is softer than $LaNi_5$ agrees with our theoretical results, the ratio is much smaller than that can be expected from our theoretical results. The reason for the underestimation is not clear. However, it may be ascribed to the formation of lattice defects during the hydrogenation process. Many kinds of lattice defects are known to be introduced in the hydrogenation process.

4. Discussion

4.1. Origin of smaller elastic anisotropy in $LaNi_5H_7$

When hydrogen atoms enter the interstitial sites, electronic structures and thus chemical bonding should be changed. In the previous section, we found that the elastic anisotropy became smaller when hydrogen atoms are accommodated. It is natural that this difference is related to the changes in the bonding by the hydrogenation. In this section we discuss the electronic mechanism.

Formation of chemical bonds can be visualized by plotting the difference between a self-consistent charge density of a compound and the sum of charge densities of isolated atoms constituting the compound. The charge differences in two crystals are shown in figure 2. They are shown as the contour map on a $(11\bar{2}0)$ plane and the three-dimensional iso-surface plot. In the figure of atomic arrangement of $LaNi_5H_7$, different hydrogen sites are denoted by t_1, t_2, and o. They are the same notation as we used previously [5]. We can see $LaNi_5$ has its charge accumulated in the hexahedral cage comprised of Ni atoms. This charge is distributed along the *c*-axis. This indicates that the Ni–Ni bond is stronger along the *c*-axis than that on the *ab*-plane. This should be the electronic mechanism behind the strong elastic anisotropy of $LaNi_5$.

On the other hand, electrons are distributed spherically and centred at the hydrogen atoms in the hydride. As the trade-off, the charge in the Ni cage is diminished. In other words, the charge accumulated within the Ni sub-lattice of $LaNi_5$ is transferred and redistributed spherically around the H atoms in $LaNi_5H_7$. The charge distribution of the hydride is no longer anisotropic along the *c*-axis. The change in the charge distribution due to the hydrogenation suggests that Ni–Ni bonds with strong directionality are weakened to make Ni–H bonds that have little directionality. This should be responsible for the smaller elastic anisotropy in $LaNi_5H_7$. The differences in the chemical bondings will be quantitatively discussed later.

As for the bonds of $LaNi_5H_7$, a TB-LMTO (tight-binding linearized muffin-tin orbitals) study has been reported by Nakamura *et al* [14]. They found that the bond energy of the interstitial hydrogen can be well described within the second moment approximation, suggesting that the directionality of bonding could be smeared out in $LaNi_5H_7$. The present results confirm their hypothesis. However, no comparison has thus far been made between $LaNi_5$ and $LaNi_5H_7$. Elastic constants have also not been discussed.

4.2. Inner displacements associated with the deformation of $LaNi_5H_7$

We have found that inner displacements in $LaNi_5H_7$ considerably reduce the calculated elastic constants. A simple way to evaluate the magnitude of the inner displacements is to take into account the bond lengths before and after the inner displacements, i.e., d^*_{AB} and d_{AB}. The

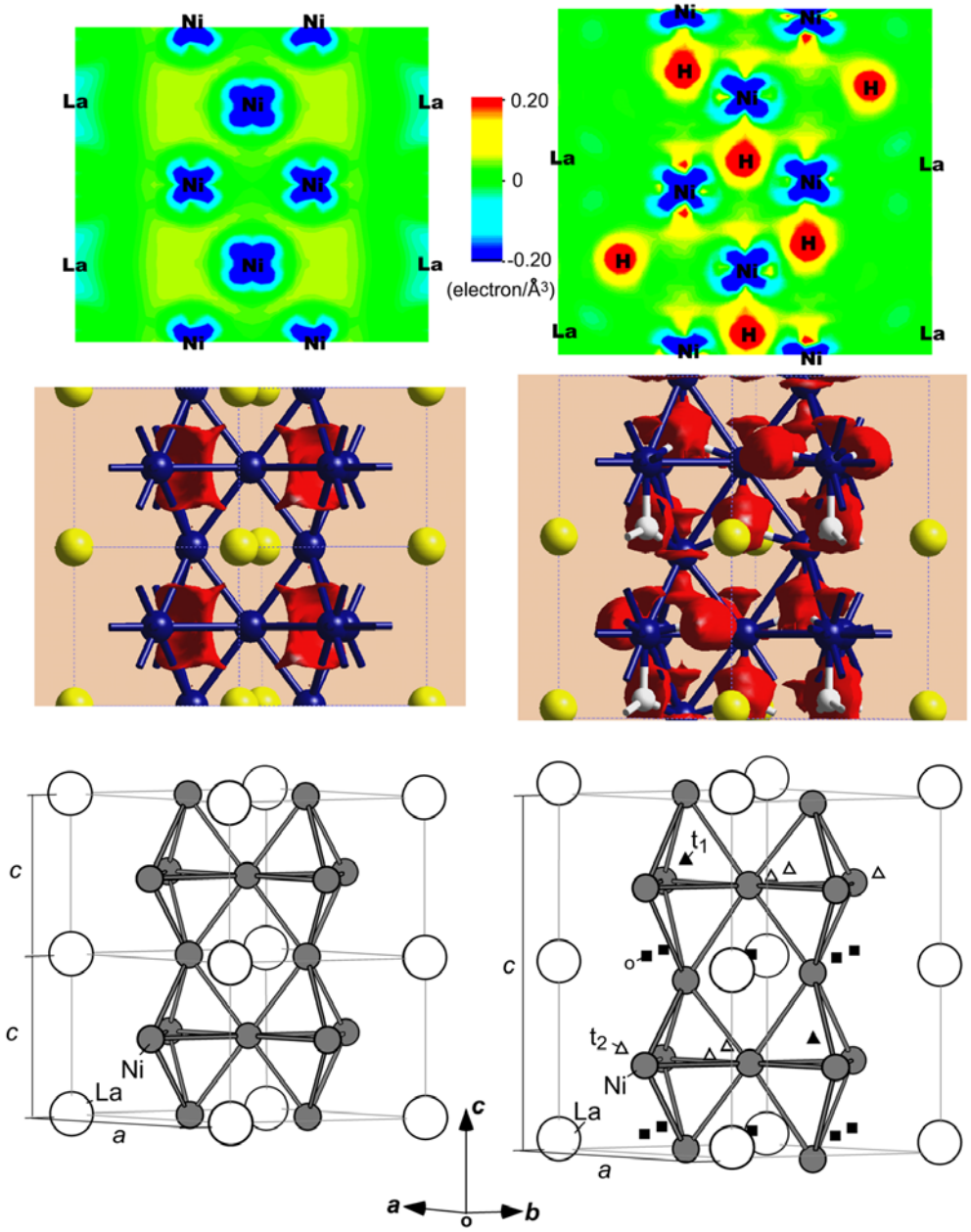

Figure 2. The spatial distribution of bonding charge for (left) $LaNi_5$ and (right) $LaNi_5H_7$. The top panels are contour maps on a $(11\bar{2}0)$ plane, while the middle panels are three-dimensional iso-surface plots (iso-value at 0.05 electrons $Å^{-3}$). The bottom panels show the corresponding atomic arrangements.

(This figure is in colour only in the electronic version)

original bond length before the deformation is denoted by d^0_{AB}. The magnitude of the inner displacement can then be characterized as $d_{AB} - d^*_{AB}$ for example. If the inner displacement

Table 2. Two parameters of inner displacements, λ_{AB} and ζ_{AB} as compared with the reduction of the elastic constants due to inner displacements, ΔC.

Deformation mode	$\Delta E/V$ to $O(\alpha^2)$	λ_{NiNi}	λ_{NiLa}	λ_{NiH}	λ_{LaH}	ζ_{NiNi}	ζ_{NiLa}	ζ_{NiH}	ζ_{LaH}	ΔC (GPa)
					$LaNi_5H_7$					
# 1	$C_{11}+C_{12}$	0.03	0.02	−0.37	0.21	0.00	−0.03	0.44	0.02	−50
# 2	$C_{33}/2$	0.00	−0.02	−0.10	0.00	0.00	—	0.43	−0.01	−21
# 3	$C_{11}-C_{12}$	0.00	0.03	−0.24	0.00	0.00	−0.03	0.67	−0.02	−30
# 4	$2C_{44}=2C_{55}$	0.04	−0.08	−0.09	−0.05	−0.01	0.23	0.76	0.26	−34
# 5	$C_{11}+2C_{33}+C_{12}-4C_{13}$	0.04	−0.02	−1.26	−0.31	0.01	0.07	0.83	0.18	−185
# 6	$9/2B$	0.02	−0.07	−0.25	0.41	0.00	0.04	0.19	−0.17	−46
					$LaNi_5$					
# 1	$C_{11}-C_{12}$	0.00	−0.01	—	—	0.00	0.01	—	—	−1
# 2	$2C_{44}=2C_{55}$	0.00	0.00	—	—	0.00	0.00	—	—	0

takes place in order to release the energy expense associated with bond expansion or contraction, d_{AB} may be close to d^0_{AB}. As a result, $d_{AB}-d^*_{AB}$ may approach $d^0_{AB}-d^*_{AB}$. A pioneering work on evaluating the inner displacement was performed by Kleinman for the diamond-type structure under trigonal strain [34]. He defined an internal strain parameter ζ. According to his definition, $\zeta=1$ corresponds to the case with rigid bond length, i.e., $d_{AB}=d^0_{AB}$, whereas $\zeta=0$ means no inner displacement, i.e., $d_{AB}=d^*_{AB}$. Applying Kleinman's idea to our crystals, which have more complicated structures and many kinds of bonds, we newly define a parameter ζ_{AB} as

$$\zeta_{AB}=\frac{1}{n_{AB}}\sum_{i=1}^{n_{AB}}\frac{d_{AB,i}-d^*_{AB,i}}{d^0_{AB,i}-d^*_{AB,i}}, \tag{10}$$

where n_{AB} is the number of bonds. This parameter provides information on the average inner displacement of each bond. Some bonds do not change their length even before the inner displacements, i.e., $d^*_{AB,i}=d^0_{AB,i}$. Those bonds having $(d^*_{AB,i}-d^0_{AB,i})/d^0_{AB,i}$ smaller than 0.5% were eliminated from the summation in equation (10) in order to avoid numerical errors.

The parameter ζ_{AB} is defined entirely from the viewpoint of bond length. In order to enable comparison with the elastic constants, a parameter having the same dimension as the elastic constants may be more useful. The energy associated with the deformation of each bond is proportional to the squared strain, i.e., $[(d_{AB}-d^0_{AB})/d^0_{AB}]^2$. The relaxation energy due to the recovery of the bond length can therefore be related to the difference between $[(d_{AB}-d^0_{AB})/d^0_{AB}]^2$ and $[(d^*_{AB}-d^0_{AB})/d^0_{AB}]^2$. The average value for the AB bond, as defined by

$$\lambda_{AB}=\frac{1}{\alpha^2}\frac{1}{n_{AB}}\sum_{i}^{n_{AB}}\left[\left(\frac{d_{AB}-d^0_{AB}}{d^0_{AB}}\right)^2-\left(\frac{d^*_{AB}-d^0_{AB}}{d^0_{AB}}\right)^2\right], \tag{11}$$

may be comparable to the reduction of the elastic constants, assuming linear elasticity for each bond.

Two kinds of parameters ζ_{AB} and λ_{AB} are calculated for the six deformation modes given by equations (2)–(7). The results are shown in table 2. Here we consider the Ni–Ni, Ni–H, Ni–La and La–H bonds within lengths of 2.80, 1.70, 3.30 and 2.80 Å, respectively. The elastic constants and their coefficients corresponding to the deformation modes are chosen such that all deformations can be scaled by the same strain α. ζ_{AB} and λ_{AB} in table 2 are average values calculated with $\alpha=+1$ and -1%. As can be seen in table 2, the inner displacements occur

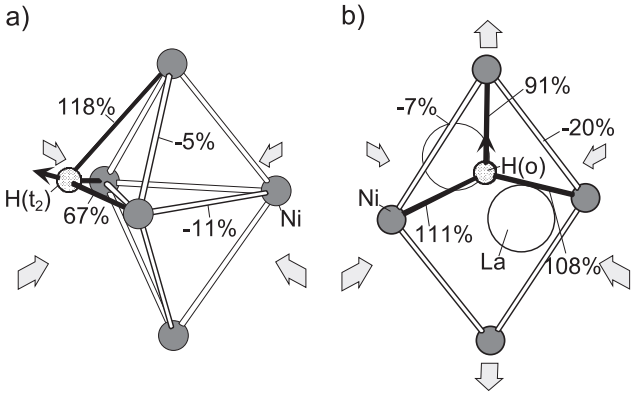

Figure 3. Changes in bond lengths associated with two kinds of deformation mode as shown by Kleinman's parameter, ζ. (a) Deformation mode of #1 $C_{11} + C_{12}$ and (b) that of #5 $C_{11} + 2C_{33} + C_{12} - 4C_{13}$ with the strain parameter $\alpha = -1\%$.

mostly on the Ni–H bonds and, to a lesser extent, on the La–H bonds. It is interesting that little inner displacement takes place for the Ni–Ni bonds for all kinds of deformation modes. The Ni–La bonds also show only small displacements. The reduction of elastic constants due to the inner displacements, ΔC, is also shown in table 2. A good correlation can be seen between λ_{NiH} and ΔC. Although some non-negligible values can be seen in λ_{LaH}, the correlation between λ_{LaH} and ΔC is much worse. On the other hand, the correlation of ΔC with ζ_{NiH} is worse than that with λ_{NiH}. Nor is there a good correlation between ζ_{LaH} and ΔC. For $LaNi_5$, both Ni–Ni and Ni–La bonds show very small displacements, in agreement with small ΔC. Changes in bond length associated with two kinds of deformation modes are shown in figure 3. Gray arrows indicate the direction of external strains. Kleinman's parameter, $\zeta = (d - d^*)/(d^0 - d^*)$, is shown for the bonds near hydrogen. In figure 3, rigid bonds with $\zeta > 50\%$ are highlighted by thick sticks. According to the definition, $\zeta = 0$ when no inner displacement takes place. $\zeta = 100\%$ when significant inner displacement occurs to recover the displacement by the external stress. In other words, $\zeta = 100\%$ when the bond is perfectly rigid. All rigid bonds are those of Ni–H. All Ni–Ni bonds are found not to be rigid. They deform so as to follow the external strain. The relative displacements of hydrogen atoms due to the inner displacement are denoted by black arrows. They are drawn under the condition that the centres of the metal atoms are set at the same position before and after the inner displacements. Hydrogen atoms move so as to keep the Ni–H bond length unchanged.

The present results show that the inner displacements of $LaNi_5H_7$ associated with the deformation are predominantly due to the movement of hydrogen atoms. The reduction in the elastic constants due to these inner displacements can be mainly ascribed to the relief of strain energy in the Ni–H bonds. They clearly indicate that the Ni–H bonds play major roles in determining elastic properties and therefore bonding mechanism of $LaNi_5H_7$. In the next section, we evaluate the magnitude of chemical bond strength on the basis of atomic orbital representation.

4.3. Chemical bondings of $LaNi_5$ and $LaNi_5H_7$

It has been suggested that the formation of Ni–H bonds plays a major role in both the disappearance of the elastic anisotropy and the inner displacements. Intuition of chemical bondings can be clearly given when wavefunctions are described by the linear combination

of atomic orbitals. The magnitude of covalent bond strength can be given by bond overlap populations following Mulliken's method [35]. In principle, wavefunctions described by plane-wave basis sets can be projected to any kind of atomic orbital set. In the present study, however, we have adopted a different set of calculations using a first principles cluster method. We have a lot of experience in analysing chemical bondings of many kinds of compound including a series of transition metal compounds by this method [36]. The abundance of systematic calculations using this method provides us with confidence in the reliability of the population analysis.

In the present study, we have employed model clusters composed of approximately 70 metal atoms. First principles calculations were made, using the program code SCAT [37]. This uses local density approximation (LDA) and numerical atomic orbitals as basis functions. The density of states (DOS) was obtained by summing local partial densities of states of atoms located at the centre of the cluster. The overlap population diagram (OPD) for the A–B bond can be obtained by plotting an overlap population at each energy level. Both DOS and OPD were obtained using a Gaussian function of 1.0 eV FWHM to broaden discrete eigenvalues and are shown in figure 4.

We compared the strength of covalent bonding between $LaNi_5$ and $LaNi_5H_7$ using the following quantity:

$$\rho_{AB} = \frac{1}{V}\sum_i N_{AB(i)} Q_{AB(i)}, \tag{12}$$

which is called the covalent bond density [36]. In equation (12), $N_{AB(i)}$ is the number of A–B bonds in the unit cell at the ith nearest-neighbour distance, $Q_{AB(i)}$ is the bond overlap population of the bonds, and V is the unit cell volume. The summation was performed for bonds having $Q_{AB(i)} > 0.01$. Figure 5 shows the covalent bond density for two crystals. It is seen that the covalent bond density of the Ni–Ni bond decreases significantly from 0.055 to 0.025 $Å^{-3}$ with hydrogenation. As a trade-off with the loss of the Ni–Ni bonds, the Ni–H bonds show the greatest contribution to the total covalent bond density of $LaNi_5H_7$. Both La–La and La–H bonds contribute little. This result is consistent with the hypothesis used in our previous paper [5] in which the preferable H-sites in the $LaNi_5$–H systems were discussed. The contributions of La 4f–Ni 3spd, La 4f–La 4f5d6sp and La 4f–H 1s interactions to ρ_{LaNi} and ρ_{LaH} were calculated to be 2 and 1% for $LaNi_5$ and $LaNi_5H_7$, respectively. These contributions are so small that the inclusion of La 4f states (which are ignored in the PWPP calculations) within the LCAO method should not significantly affect the covalent density analysis in figure 5.

In the DOS of $LaNi_5H_7$, the valence band shows two regions. H 1s states can be found in the lower part of the valence band centred at -7 eV. Small contributions of Ni 3d and Ni 4sp orbitals can be found in the lower valence band. The upper part of the valence band is mainly composed of Ni3d states. The contribution of H 1s to the upper valence band is very small. These features of the valence band DOS agree with previous LMTO-ASA results [11]. La 4f states are almost unoccupied and strongly localized around 2 eV above E_F, which is consistent with their small contribution to the covalent bond density.

The OPDs in figure 5 provide detailed information on interactions between the orbitals. Ni and H strongly interact in a bonding manner in the lower valence band. Bonding between Ni–Ni and Ni–La can be seen in the upper valence band. When the OPD of Ni–Ni for the hydride is compared with that of the host, we can see that the magnitude of the Ni–Ni bonds is markedly reduced even in the upper valence band below -3 eV. This is the reason for the decrease in the covalent bond density of Ni–Ni in the hydride.

From the investigation on the chemical bond strength in the two compounds, we found clear evidence that the major bonds are changed from Ni–Ni to Ni–H by the hydrogenation. This

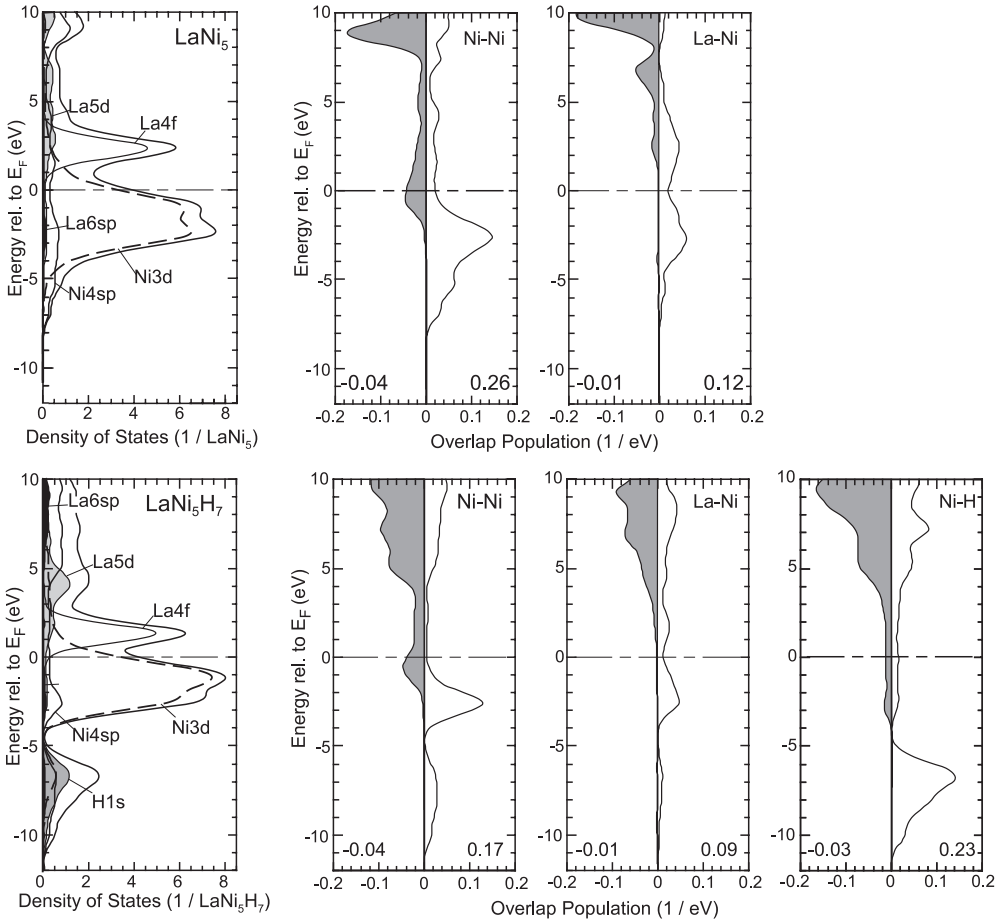

Figure 4. Total and partial density of states and OPD of (top) $LaNi_5$ and (bottom) $LaNi_5H_7$ obtained by the molecular orbital method. The OPDs are shown for Ni–Ni and La–Ni bonds in $LaNi_5$, and for Ni–Ni, La–Ni and Ni–H bonds in $LaNi_5H_7$. In the OPD right-hand and left-hand sides of the horizontal axis indicate bonding and anti-bonding interactions, respectively.

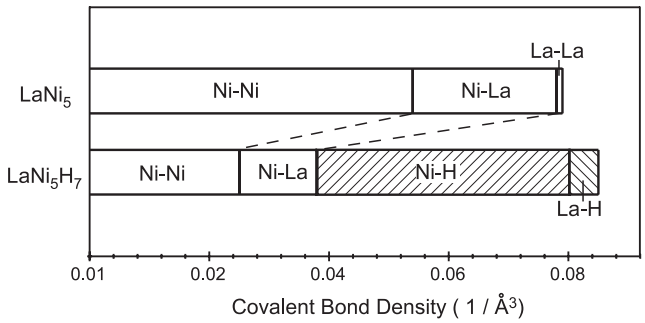

Figure 5. Covalent bond densities in $LaNi_5$ and $LaNi_5H_7$ obtained using molecular orbital calculations.

strongly supports the discussion on the changes in the elastic constants during hydrogenation given in the previous sections. In section 4.1, we have discussed the elastic anisotropy from

the viewpoint of the charge distribution. Electronic charge accumulated in the interstices of the Ni sub-lattice of $LaNi_5$ is transferred and redistributed around the H atoms in the hydride. The charge redistribution is consistent with the change in dominant bonds. In section 4.2, we found a good correlation between the inner displacements of Ni–H bonds, λ_{NiH}, and the decrements of elastic constants, ΔC. The reduction in the elastic constants due to the inner displacements can be predominantly ascribed to the movement of hydrogen atoms to relieve the strain energy in the Ni–H bonds. The large covalent bond density of Ni–H in the hydride, as found in this section, should account for the considerable energy relief.

5. Conclusions

We have used an *ab initio* pseudopotential method with a plane wave basis to investigate the elastic properties of $LaNi_5$ and its hydride. Our results can be summarized as follows.

(1) All independent elastic constants of $LaNi_5$ and its hydride, $LaNi_5H_7$, were calculated from the total energy–strain curves. The absolute values of the calculated elastic constants of $LaNi_5$ were systematically greater than the experimental values by 10–18%. However, the relative values among C_{ij} s were in satisfactory agreement.
(2) The elastic anisotropy in $LaNi_5$ is found to be diminished in its hydride. In $LaNi_5$, charge is found to be accumulated in the interstices of the Ni sub-lattice, which is distributed along the *c*-axis. This indicates that the bonding in $LaNi_5$ is stronger along the *c*-axis than on the *ab* plane. On the other hand, in $LaNi_5H_7$, electrons are distributed much more spherically centred at the hydrogen atoms. This is proposed to be the electronic mechanism behind the smaller elastic anisotropy in $LaNi_5H_7$ as compared to $LaNi_5$.
(3) Inner displacements associated with external strain were found to be significant only in $LaNi_5H_7$. Without inclusion of the inner displacement, elastic constants cannot be evaluated properly. Detailed analysis of the bond lengths in deformed crystals revealed that hydrogen atoms located at low-symmetry sites move in order to maintain the Ni–H bond lengths during deformation. Little inner displacement can be found for Ni–Ni and Ni–La bonds even in $LaNi_5H_7$. The reduction of the elastic constants due to the inner displacements can be well correlated with the magnitude of the inner displacements.
(4) An extra set of first principles cluster calculations were made in order to evaluate the magnitude of chemical bondings in $LaNi_5$ and $LaNi_5H_7$. Ni–H bonds were found to be dominant in $LaNi_5H_7$ as a result of a trade-off with Ni–Ni and Ni–La bonds in $LaNi_5$. This result is consistent with our discussion on the origin of smaller elastic anisotropy as well as the origin of inner displacements in $LaNi_5H_7$.

Acknowledgments

We would like to thank Dr F Oba for helpful discussions. This work was supported by Grant-in-Aids for Scientific Research on Priority Areas (No 751) from MEXT Japan.

References

[1] Willems J J G and Buschow K H J 1987 *J. Less-Common Met.* **129** 13
[2] van Vucht J H N, Kuijpers F A and Bruning H C A M 1970 *Philips Res. Rep.* **25** 133
[3] Schlapbach L (ed) 1988 *Hydrogen in Intermetallic Compounds I* (*Topics in Applied Physics* vol 63) (Berlin: Springer)
Schlapbach L (ed) 1992 *Hydrogen in Intermetallic Compounds II* (*Topics in Applied Physics* vol 67) (Berlin: Springer)

[4] Lartigue C, Le Bail A and Percheron-Guegan A 1987 *J. Less-Common Met.* **129** 65
[5] Tatsumi K, Tanaka I, Inui H, Tanaka K, Yamaguchi M and Adachi H 2001 *Phys. Rev.* B **64** 184105
[6] Tanaka K, Okazaki S, Ichitsubo T, Yamamoto T, Inui H, Yamaguchi M and Koiwa M 2000 *Intermetallics* **8** 613
[7] Malik S K, Arlinghaus F J and Wallace W E 1982 *Phys. Rev.* B **25** 6488
[8] Gupta M 1987 *J. Less-Common Met.* **130** 219
[9] Suenobu T, Tanaka I, Adachi H and Adachi G 1995 *J. Alloys Compounds* **221** 200
[10] Yukawa H, Matsumura T and Morinaga M 1999 *J. Alloys Compounds* **293–295** 227
[11] Nakamura H, Nguyen-Manh D and Pettifor D G 1998 *J. Alloys Compounds* **281** 81
[12] Gupta M 2000 *J. Alloys Compounds* **293–295** 190
[13] Szajek A, Jurczyk M and Rajewski W 2000 *J. Alloys Compounds* **307** 290
[14] Nakamura H, Nguyen-Manh D and Pettifor D G 2000 *J. Alloys Compounds* **306** 113
[15] Milman V, Winkler B, White J A, Pickard C J, Payne M C, Akhmatskaya E V and Nobes R H 2000 *Int. J. Quantum Chem.* **77** 895
[16] Wernick J H and Geller S 1959 *Acta Crystallogr.* **12** 662
[17] Perdew J P, Chevary J A, Vosko S H, Jackson K A, Pederson M R, Singh D J and Fiolhais C 1992 *Phys. Rev.* B **46** 6671
[18] Vanderbilt D 1990 *Phys. Rev.* B **41** 7892
[19] Milman V and Winkler B 2001 *Z. Kristallogr.* **216** 99
[20] Monkhorst H J and Pack J D 1976 *Phys. Rev.* B **13** 5188
[21] Beckstein O, Klepeis J E, Hart G L W and Pankratov O 2001 *Phys. Rev.* B **63** 134112
[22] Ravindran P, Fast L, Korzhavyi P A and Johansson B 1998 *J. Appl. Phys.* **84** 4891
[23] Holm B and Ahuja R 1999 *J. Chem. Phys.* **111** 2071
[24] Wright A F 1997 *J. Appl. Phys.* **82** 2833
[25] Shimada K, Sota T and Suzuki K 1998 *J. Appl. Phys.* **84** 4951
[26] Sörgel J and Sherz U 1998 *Eur. Phys. J.* B **5** 45
[27] Stadler R, Wolf W, Podlocky R, Kresse G, Fürthmuller J and Hafner J 1996 *Phys. Rev.* B **54** 1729
[28] Chetty N, Muñoz A and Martin R M 1989 *Phys. Rev.* B **40** 11934
[29] Nielsen O H and Martin R M 1985 *Phys. Rev.* B **32** 3792
[30] Ficher T H and Almlof J 1992 *J. Phys. Chem.* **96** 9768
[31] Tanaka K and Koiwa M 1999 *High Temp. Mater. Proc.* **18** 323
[32] Nye J F 1985 *Physical Properties of Crystals* (New York: Oxford University Press)
[33] Bereznitsky M, Ode A, Hightower J E, Yeheskel O, Jacob I and Leisure R G 2002 *J. Appl. Phys.* **91** 5010
[34] Kleinman L 1962 *Phys. Rev.* **128** 2614
[35] Mulliken R S 1955 *J. Chem. Phys.* **23** 1833
[36] Mizuno M, Tanaka I and Adachi H 1999 *Phys. Rev.* B **59** 15033
[37] Adachi H, Tsukada M and Satoko C 1978 *J. Phys. Soc. Japan* **45** 875